REVIEW: HYDRO-, MICRO- AND NANOGELS STUDIED BY COMPLEMENTARY MEASUREMENTS BASED ON SEM AND SFM.

Matzelle, T.[1]*, Reichelt, R.[2]

[1]Chimie-Physique des Matériaux, Université Libre de Bruxelles, B-1050 Bruxelles, Belgium
[2]Institut für Medizinische Physik und Biophysik, Universitätsklinikum, Westfälische Wilhelms-Universität, Münster, Germany

*Corresponding author: matzelle@ulb.ac.be

Received: March 11th, 2008. Accepted: May 2nd, 2008
Published on-line: May 30, 2008

ABSTRACT
The research on soft materials is interdisciplinary. In the present work we focus on "smart hydrogels" as most promising representatives studied by complementary Scanning Force Microscopy (SFM) and high resolution Scanning Electron Microscopy (SEM). The extremely large range of water uptake of these hydrogels (up to 10^3 times of their mass) on one hand and their distinct softness (Young´s modulus < some tens of kPa) on the other hand constitute real challenges for the characterization of their local structure, the caging of nano-scaled particles, and some micromechanical properties. SFM images were compared with those obtained by SEM in the dry, swollen and deswollen state of the "smart gel" PNIPAAm [poly-(N-isopropylacrylamide)]. PNIPAAm reacts on tiny variations of the temperature around 33°C by significantly changing its volume. While both imaging techniques revealed very similar results concerning the surface structure in the dry state, highly resolved structural features remained unapproachable for SFM in the wet state. In a contrary, SEM at high resolution revealed after state-of-the-art cryo-preparation, freeze-drying and subsequent ultrathin Pt/C-coating a sponge-like structure with cavity sizes of around 40 nm in the swollen state and 20 nm in the deswollen state. SFM proved to be an appropriate instrument revealing the local elastic surface properties. For example, at the swollen state at 10 °C, the Young's modulus was found to be more than 100 times lower than for the deswollen state at 35 °C. In addition, SEM also proved to be very suitable for the structural research of microgels and filled hydrogels. The application of both SFM and SEM contribute complimentarily to a characterization of different hydrogel systems at different states.

Keywords: SFM, SEM, hydrogels, microgels, Young´s modulus

RESUMEN
La investigación en materiales blandos es interdisciplinaria. En este trabajo nos concentraremos en "hidrogeles smart" como representantes más prometedores estudiados complementariamente por Microscopía de Fuerza Atómica (MFA) y Microscopía Electrónica de Barrido (MEB) de alta resolución. Los hidrogeles muestran una alta capacidad de absorción de agua (hasta 10^3 veces su masa) y un amplio rango de propiedades mecánicas (Módulo de Young < algunas decenas de KPa). El estudio sistemático de estas propiedades y su estrecha relación con la microestructura constituyen un verdadero desafío para la caracterización de su estructura local, la incorporación y distribución de nanopartículas en su estructura interna y algunas propiedades micromecánicas. En esta revisión se hace un análisis comparativo de imágenes obtenidas desde SFM y SEM del "smart gel" PNIPAAm [poli-(N-isopropil-acrilamida)] en estado xerogel, hinchado y deshinchado. El PNIPAAm modifica significativamente su volumen ante pequeñas variaciones de temperatura alrededor de 33 ºC. Mientras ambas técnicas revelaron resultados muy similares relativos a la estructura superficial en el estado seco, las características estructurales de mayor resolución han permanecido inalcanzables para el SFM en estado húmedo. Al contrario, el SEM a alta resolución después de una crio-preparación, congelación-secado y subsiguienre deposición de una capa ultrafina de Pt/C, revela una estructura esponjosa con cavidades de dimensiones cercanas a los 40 nm en su estado hinchado y 20 nm en el estado deshinchado. SFM ha demostrado ser un instrumento apropiado para revelar las propiedades locales elásticas superficiales. Por ejemplo, en el estado hinchado a 10 ºC, el módulo de Young era más de 100 veces el del estado deshinchado a 35 ºC. Adicionalmente, SEM ha demostrado ser muy adecuado para la investigación estructural de microgeles e hidrogeles nanoestructurados. La aplicación de SFM y SEM contribuyen complementariamente a la caracterización de diversos sistemas de hidrogeles en diferentes estados.

INTRODUCTION

Soft materials have a wide range of applications such as foams, lubricants, adhesives, rubbers, gels and cosmetics. In contrast to this wide variety of appearances, their basic characteristics exhibit common physico-chemical origins. For example, the weak interaction between their

structural elements is one obvious key feature. On the macroscopic level the weak interactions cause softness which plays an important role in areas such as medical care, medicine, foods, and bioengineering. In case of polymer gel as a major representative of soft matter, softness arrives from a cross-linked three-dimensional network capable to absorb solvent to a high degree without dissolution. If the solvent is water the gel is termed hydrogel. Hydrogels are water swollen, cross-linked polymeric structures produced by the simple reaction of one or more monomers or by association of bonds such as hydrogen bonds and strong van der Waals interactions between chains. These systems exist in a state between solid and liquid. This feature sets them apart from other forms of matter. Innovative research and development is growing ever since. Presently, a huge number of synthetic hydrogels is known. For instance, they are applied as soft contact lenses [1], drug delivery systems (DDS) [2–5], medical sensors [6], biocompatible materials for plastic surgery [7], sanitary products like disposal diapers [8], or separation matrices like molecular sieves and adsorption resins [9]. However, a large amount of today's research is focused on probably the most interesting hydrogels, the so-called "smart" or "intelligent" hydrogels. A representative of this interesting class of hydrogels is a polymer system with a defined phase transition capable to abruptly swell to many times its original size or to collapse into a compact mass when stimulated externally [3].

Smart hydrogels react in response to an external stimulus in a manner similar to many living organisms rather than to not living organic matter [10]. Some systems are reported to sense environmental changes such as an electric field [11], pH [12,13], temperature [13–16], salt content and solvent composition [17]. In response to these external stimuli they undergo a reversible phase transition leading to changes in their macroscopic size, optical appearance or elastic modulus (see Fig. 1).

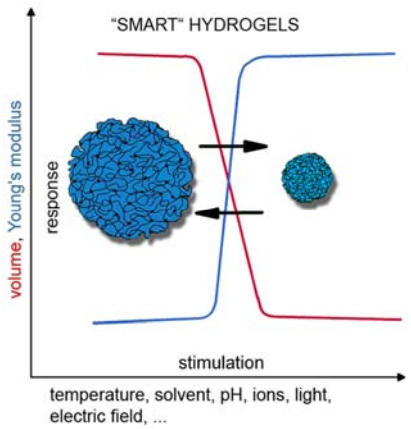

Fig. 1: Scheme of the stimulated response of a "smart" hydrogel.

The unique properties of these soft materials have led to serious efforts in medical research and bioengineering, especially regarding the development of self-regulating drug delivery systems [18,19], on-off switches for enzymatic reactions [20], biosensors [21], purification matrices [22,23] and biomedical actuators [24,25]. Some basic fields of application are schematically presented in Fig. 2. For a detailed view on modern applications of smart hydrogels in medicine and biology see Peppas et al. [26].

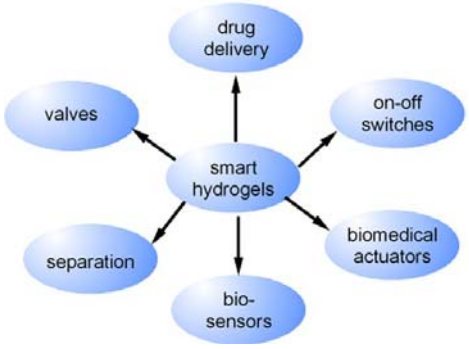

Fig. 2: Basic fields of application of smart hydrogels.

Common for most applications is that they take advantage out of a sharp phase transition with distinct changes in network structure stimulated by a marginal change of the environmental conditions. This may be explained physico-chemically on the basis of P. J. Flory's theory [27]. However, the investigation methods of the steep volumetric phase transition in soft polymeric gels

were mainly on macroscopic scale. For example, extensive macroscopic studies were performed due to temperature changes [28], the influence of the initial monomer concentration [29], heavy water [30] and the synthesis temperature [31].

Although numerous macroscopic studies were performed with various hydrogels over the past years, quantitative reports of microscopic investigations are still quite scarce. However, modern microscopic methods are gaining significant importance in gel research. For example, the number of publications reporting on SEM investigations of hydrogels has impressively increased from 11 in the year 1990 to 207 in 2006 as shown in the figure 3. Interestingly, the number of publications reporting on "SFM" or "AFM" *(Atomic Force Microscopy)* investigations of hydrogels is very small and did not increase significantly within the period of time considered.

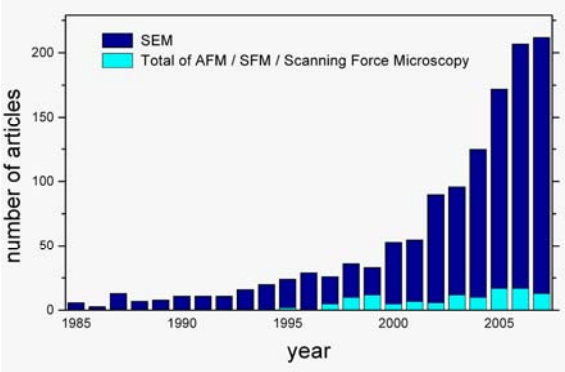

Fig. 3: The figure shows the number of articles published per year in regard of the keywords "hydrogel" and "SEM" or "hydrogel" and ("AFM" or "SFM" or "Scanning Force Microscopy"). The results are based on a SciFinder Scholar search.

For many new applications and in spite of the prospect of polymer gels playing an essential role in the solution of global problems such as environmental pollution and limited food resources, there is a growing need for a detailed understanding of the properties of hydrogels at a microscopic and nanoscopic scale. This work is aimed to review contributions by SEM and SFM to elucidate the microstructural and micromechanical properties of soft hydrophilic matter. Despite limiting the scope of this study to smart hydrogels, the application of SEM and SFM can be expended to any type of soft and water-containing materials.

The structure of the smart gel PNIPAAm

PNIPAAm [poly-(N-isopropylacrylamide)] is regarded to be one of the most promising smart gels being extensively studied since the early 80's. PNIPAAm undergoes a reversible volume phase transition in response to external temperature changes. Inserted in water, the polymer matrix strongly shrinks as the temperature increases above the lower critical solution temperature (LCST), which is about 33 °C. PNIPAAm hydrogel can be synthesized by free radical polymerisation (for the recipe see, e.g., Suzuki et al. [32]).

Basically the studies presented in the following are aimed to characterize the micro- and nano-structure and the micromechanical properties of PNIPAAm hydrogels above and below LCST. Two powerful microscopies, the SFM and the Field Emission Scanning Electron Microscopy (FESEM) were applied to study PNIPAAm samples in three different structural states, dry at room temperature (RT), water-swollen at RT, and deswollen at 35 °C.

Topography measurements on air-dried PNIPAAm were performed with SFM under atmospheric conditions at 20 °C and compared with those revealed by FESEM. SFM provides a rather smooth gel surface with nm-sized protrusions, similar to what is seen by FESEM (Fig. 4). FESEM measurements were performed using low acceleration voltages in order to keep the penetration power of the electrons small. Low electron doses were used to avoid beam-induced charging effects and specimen damaging. At higher irradiation doses "scan windows" appear, indicating the sensitivity of the PNIPAAm surface. In addition to laterally resolved surface structural details, the SFM images provided

quantitative topographic information: e.g., the height of the roundish protrusions varied from 5 nm to 15 nm. These protrusions may indicate regions with higher polymer density.

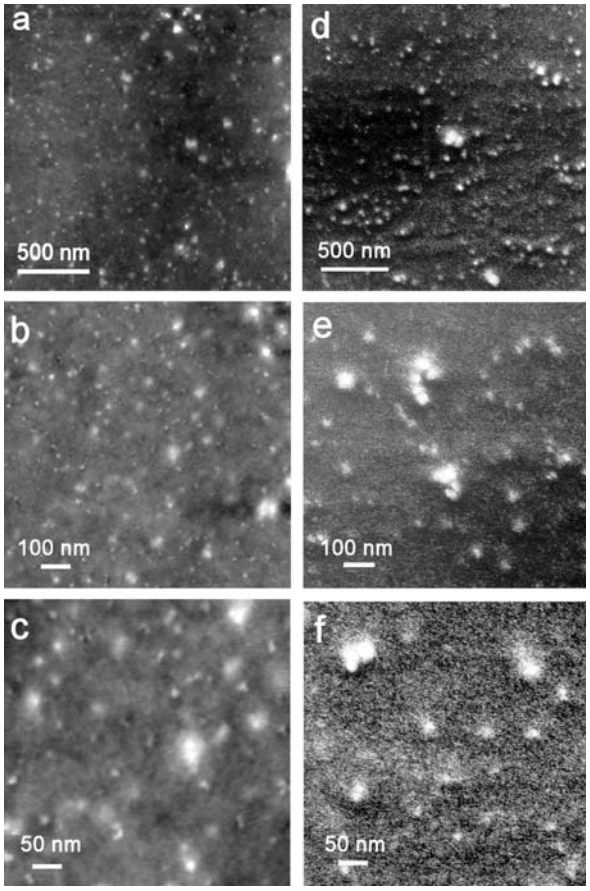

Fig. 4: IC-SFM images (a - c) and FESEM secondary electron micrographs (d - f) of the air-dried (RT) PNIPAAm gel surface. For FESEM investigations the air-dried hydrogel surface was coated with 2.5 nm Pt/C at an elevation angle of 65°. The variation in topography is 23 nm (a), 12 nm (b) and 5.3 nm (c) with bright parts indicating increased elevations. Reprinted with permission from J Phys Chem B 106:2861-2866, Copyright (2002) ACS.

In case of the water-swollen PNIPAAm surface we only received "cloudy" irreproducible topographs, despite using less invasive imaging modes. That is caused by problems associated with an imaging of soft hydrogel surfaces using high aspect ratio SFM tips with suitable cantilever spring constants. The discrimination between the indentation of the tip and the effective sample surface is crucial. Indeed, it was found that the probing tips can easily penetrate the swollen gel surface when applying relatively small forces in the order of 1 nN [33]. In this case large adhesive interaction forces were observed. This observation is in good agreement with recently published results of measurements on water-swollen microgel particles. However, significant hydrogel penetration and strong adhesion forces are found to be noticeable reduced when applying a different SFM operating mode, the so-called magnetic cantilever exitation mode (MAC mode). Hence, MAC mode SFM is proposed to be the most suitable technique for in-situ SFM studies on volume changes at microgel particles during the phase transition so far (e.g., Wiedemair et al. [34]).

To reduce the locally acting force during scanning, we replaced high aspect SFM tips by smooth glass spheres with diameters between 3–7 µm. Ducker et al. first applied a similar "colloidal-probe technique" [35,36,37]. Unfortunately, the avoidance of surface penetration using glass spheres as probes was accompanied by a significant reduction of lateral resolution during surface imaging. Thus, glass spheres were used preferentially to probe local mechanical properties of the hydrogel surface instead of probing its morphology.

FESEM combined with state-of-the art cryo-preparation techniques, in contrast to that, is a very powerful tool to study the micro- and nanostructure of PNIPAAm hydrogels below and above the LCST. Figure 5 shows the characteristic sponge-like structure at two different temperatures. Small cavities are confined by thin perforated membranes. Comparing the images of the deswollen state (35 °C) with those of the swollen state (RT) reveals a noticeable difference.

Although the SEM measurements satisfy in a precise determination of pore sizes, the high resolution SEM gains increasing importance in the determination of exact topography in a more general perspective. As SFM is restricted to height variations less than ~ 10 µm and a

scanning field smaller than ~ 100 x 100 µm², SEM enables the operator to visualize fields of bigger sizes and to locate particular details on the surface readily. Stereoscopic SEM images can be used to obtain information about topography and spatial structure as shown by a stereoscopic FESEM image of the PNIPAAm surface in figure 6.

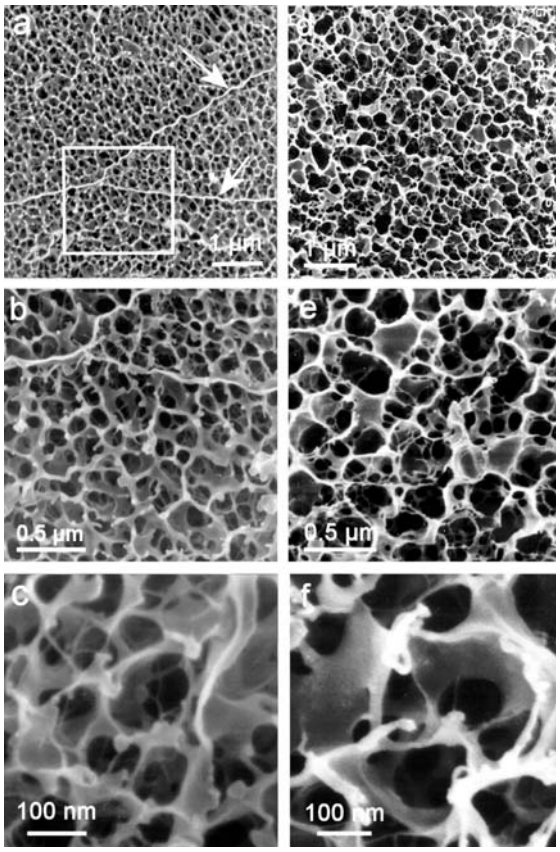

Fig. 5: FESEM secondary electron micrographs of the PNIPAAm gel surface in the deswollen state at 35 °C (a, c) and the swollen gel surface at room temperature (d–f) at different magnifications. Both states show a similar spongy structure but the mean size of cavities differs by a factor of approximately two. Reprinted with permission from J Phys Chem B 106:2861-2866, Copyright (2002) ACS.

The results shown demonstrate that SEM is best suited for investigations of hydrogel polymers. Indeed, SEM has often proven to be a very good choice in hydrogel research, in particular regarding morphological studies in the submicrometer range.

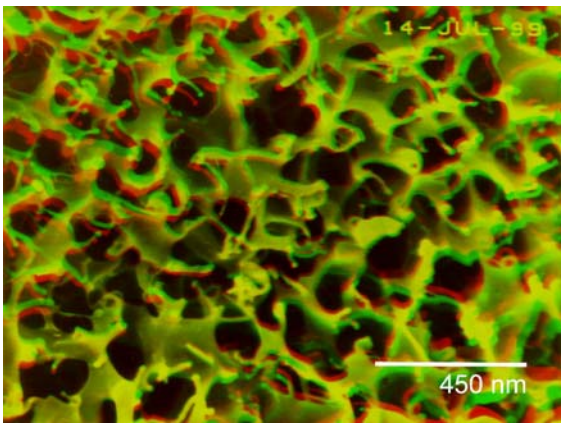

Fig. 6: Red-green stereo anaglyph of FESEM secondary electron micrographs of the PNIPAAm gel surface in the swollen state at RT. The stereo pair has been acquired by tilting the sample holder at ±6°. Courtesy of Hawkes P.W., Spence J.C.H. (2007). The Science of Microscopy, vol 1, p. 235. With kind permission of Springer Science and Business Media. [38].

Below we present two further examples of structural research on PNIPAAm hydrogels:

(i) The interior morphology of biodegradable dextran-methacrylate hydrogels can be visually examined using SEM and Mercury Intrusion Porosimetry (MIP) [39]. These two techniques are applied to obtain reliable quantitative data of pore characteristics. In this case, too, average pore sizes are determined by image analysis of SEM micrographs. Noteworthy, the swollen dextran-metacrylate hydrogel shows a different pore size and morphology at the surface and the interior.

(ii) In some applications a rapid swelling-deswelling response of PNIPAAm may be favourable. Following another polymerization recipe using the hydrophobic initiator dodecyl dimethyl benzyl ammonium bromide (DDBAB), a macroporous PNIPAAm hydrogel with ultrarapid swelling-deswelling properties was obtained by Zhao et al. [40].

Again, SEM turns out to be most suitable for visualizing the micro-morphology of gels. Interestingly, PNIPAAm gels with the presence of DDBAB during the polymerization becomes macroporous with pore sizes of about some ten times larger than for the non-DDBAB

hydrogel. The number of macropores increases for larger amounts of DDBAB. In general, higher amounts of DDBAB result in an interconnected macroporous structure with fast reversible swelling-deswelling kinetics: The time required to reversible swell to equilibrium state is about 1 minute for disks of 20 mm in diameter and 5 mm in thickness. Finally, the non-DDBAB hydrogel reveals a microporous spongy structure with pore sizes similar to our findings with PNIPAAm [41].

Micromechanical properties

The SFM is not restricted to the imaging mode only. SFM is perfectly suited to determine local mechanical properties such as Young's modul as it uses a force sensor to apply and accurately measure forces on the submicrometer scale. Local elastic properties of any sample surface can be obtained under ambient conditions in air and in water with high precision. In principle, these properties are revealed by force curves showing the indentation of the surface as the probe loads the sample. In this respect SFM is a unique instrument. It has proven its potential in pioneering studies of soft materials like cartilages, gelatine, and living cells in their natural environment [42,43,44].

The local elastic modulus of the PNIPAAm gel surface below and above the LCST was measured using the force spectroscopy mode of SFM operation. As mentioned before, the swollen hydrogel surface is as fragile to easily penetrate the surface when applying small loads. Therefore, the force sensing probe was modified by attaching an approximately 5 µm sized silica sphere to its extremity. The exact sphere diameter was measured individually from FESEM micrographs of the cantilever prior to its employment in the SFM experiment.

In Fig. 7 the measured indentation is plotted versus the loading force. Data sets are shown for six different temperatures. To do so, the forces were calculated by multiplying the cantilever deflection by the cantilever spring constant. Each data set is fitted to the Hertz model, according to the geometrical set-up of a smooth sphere and a flat surface. The Hertz model predicts a power law relation between the indentation and the loading force on a tip (Fcone) or on a sphere (Fsphere). The expressions for the indentation are given by [45,46].

$$\delta = \sqrt{\frac{2}{\pi}\frac{\left(1-\nu^2\right)}{E}\frac{F_{cone}}{\tan\alpha}}\,, \qquad (1)$$

in the most general term of a SFM tip indenting a surface (half opening angle of the used tips was $\alpha \approx 12.5°$) and

$$\delta = \left(\frac{3}{4}\frac{\left(1-\nu^2\right)}{E}\frac{F_{sphere}}{\sqrt{R}}\right)^{\frac{2}{3}}, \qquad (2)$$

in case of the cantilevers prepared by a silica sphere, where R, E and ν are the radius of the sphere, Young's modulus and the Poisson ratio. The parameters are R = 3.5 µm, ν = 0.5 and a cantilever spring constant of 0.4 N/m in each case.

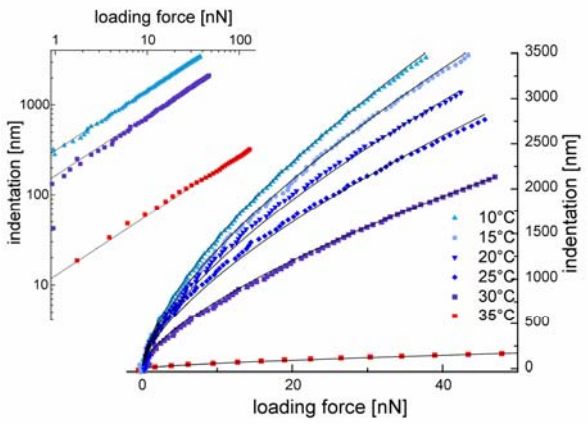

Fig. 7: The diagram shows the indentation versus the load at six different temperatures. The experimental data are represented by symbols. Each data set has been simulated using the Hertz theory for a sphere indenting a flat surface (solid lines). The Hertz theory has been used to determine the Young's modulus at each temperature. The corresponding log-log presentation is given as insert (the graphs for 15 °C, 20 °C and 25 °C are not shown for the sake of clarity). Reprinted with permission from J Phys Chem B 106:2861-2866, Copyright (2002) ACS.

The comparison between the experimental data and the prediction based on this power law reveals the value of the local Young's modulus. Quite interestingly and likely

caused by the effect of the water meniscus, the experimental retraction curves for a sharp hydrophilic tip indenting the swollen PNIPAAm surface show unusually large (100 nN) and wide-ranged (1.5 µm) "snap-back" forces.

The values of the local Young's modulus are 1.71 kPa for the swollen state at 10 °C and 4.49 kPa at 30 °C, respectively, and 183 kPa for the deswollen state at 35 °C. Thus, the local Young's modulus of a PNIPAAm gel surface is strongly affected by the phase transition occuring around 33 °C. The local stiffness is more than 100 times higher in the deswollen state at 35 °C than in the swollen state at 10 °C.

If the assumption is made that the measured homogeneous response of the water-swollen hydrogel also holds on the nanoscale we can estimate the indentation for a conical tip (half opening angle α = 12.5°) and a spherical tip with a diameter of 10 nm, 100 nm, 500 nm and 1000 nm, respectively. This situation is demonstrated schematically in Fig. 8. With Young's modulus E = 2.29 kPa (as determined for the swollen PNIPAAm gel surface at 20 °C) and a given interaction force, the indentation can be calculated from equations (1) and (2).

Since the Hertz model holds for $\delta << R$ only [47,48] the maximum loading force F_{sphere}^{max} used for a rough estimate of the indentation of a sphere with a radius R was selected such that $\delta = 0.1\ R$. The indentation δ for a very sharp tip (e.g., $2R \leq 10$ nm, cone situation) amounts 970 nm for 1 nN, about 300 nm for 0.1 nN, and approximately 100 nm for 0.01 nN. For 2R = 100 nm, 500 nm and 1000 nm (blunt tips, sphere situation) F_{sphere}^{max} amounts about 3 pN, 8 pN and 30 pN, respectively. Fig. 8 shows schematically four tips with different radii exerting nearly the same indentation into the hydrogel. This rough estimate indicates clearly that the loading force for tips with $2R \leq 1$ µm must be very small ($F << 1$ nN) in order to get an elastic response of the hydrogel surface. However, such small interaction forces are practically hardly achievable when studying a hydrogel surface in water. In addition, both, a very sharp tip penetrating the gel matrix by several hundred nm or a spherical tip with a significantly larger diameter sense a contact area with a size of at least 100 nm, i.e., high resolution SFM imaging of the swollen PNIPAAm gel surface obviously seems impossible.

The schemes in Fig. 8 denotes qualitatively the basic problem associated with the imaging of soft matter using sharp SFM tips and suitable cantilever spring constants: The lateral resolution obtainable can be judged referring to the extended contact area of the SFM tip with the soft material which depends on the elastic modulus of the sample, the tip radius, and the loading force. Hence, atomic resolution is impossible due to the unavoidable deformation of the surface during imaging. Even molecular resolution may not be achievable when applying external forces of 1pN or higher [48].

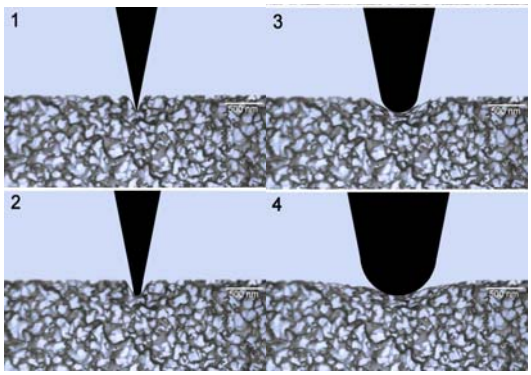

Fig. 8: Scheme of a hydrogel cross-section, being indented by a hydrophobic tip with a diameter of 10 nm (1), 100 nm (2), 500 nm (3), and 1000 nm (4).

Although SFM is not feasible to reveal high resolution structural information from soft materials, induced elastic deformation can be used to measure their local elastic properties. The above described technique for the determination of Young's modulus has become a standard procedure today. It is routinely applicable for probing mechanical surface properties on both rigid materials such as titanium implants [49] and soft matter

like cells, gels and tissues [45]. However, Jacot et al. introduced an instrument that is less complex and less expensive than the SFM dedicated for microindentation experiments based on the above mentioned technique (but note: there is no imaging capability!). Obviously, the instrument works also with very soft materials as shown with measurements of Young's modulus on polyacrylamide (PAAm) hydrogels ranging from 2.6 to 40 kPa [50]. These results are in reasonable agreement with those revealed on PAAm with higher crosslinker concentration (98 to 470 kPa), published by Matzelle et al. [51].

Microgels

One of the main findings in the structural analysis of wet hydrogels is their spongy-like appearance. The open system morphology allows hydrogels to absorb, transport and release different materials. The occurrence of a phase transition depends on how the open structure interacts with the environment. The swelling-deswelling-behaviour controlled by a physical or a chemical signal is strongly time-dependent. For most applications a quick signal response is wanted. As the hydrogel's swelling-deswelling-kinetics depends on the gel size, the dimensions are to be reduced, if fast response times are needed. One method of realizing fast response times is to reduce hydrogel sizes by preparing thin gel layers. For example, thin layers of PNIPAAm may be synthesized with the copolymer photo-crosslinked to 2-(dimethylmaleinimido)-N-ethylacrylamide (DMIAAm) [52]. Another approach in creating small sized hydrogels is the synthesis of microgel particles, based on different crosslinking techniques [53,54]. The gel particles created show almost spherical shape and fast swelling/deswelling kinetics. Other polymerisation methods are based on electron beam- or γ-irradiation of the aqueous polymer solution above LCST [55,56]. The advantage of these "clean" polymerization methods is an additive-free crosslinking process, i.e., no initiator, crosslinker, accelerator etc. are needed.

Next, SEM shows to be feasible for the structural characterization of microgels. For example, the structure of PNIPAAm microgels and poly(venyl-methyl-ether) (PVME) microgels was studied in detail by Reichelt et al. using FESEM and cryo-prepared samples (Fig. 9) [56]. The PVME microgel particles showed in the swollen state at 25 °C an almost spherical shape with a creased surface and a spongy internal structure. The outer diameter of particles was in the range of 250 – 450 nm and their surfaces sporadically revealed small holes of about 10 nm. The incidence of an irregular polymeric net that can be found between the microgels may be assigned to the imperfectly crosslinked polymers in solution.

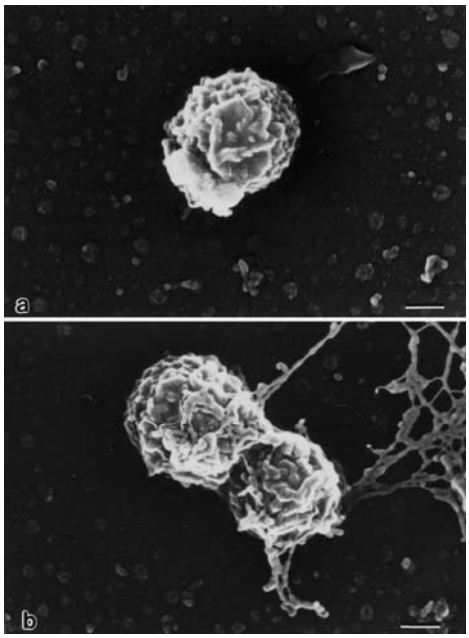

Fig. 9: PVME microgels synthesized by crosslinking the phase separated structure of diluted polymer solutions with electron beam irradiation. The images were recorded by FESEM with secondary electrons using freeze-dried samples in the swollen state at 25 °C (a) and in the deswollen state at 40 °C (b). The scale bars correspond to 100 nm. Reprinted with permission from Macromol Symp 210:501-511, R. Reichelt et al. Copyright (2004) Wiley-VCH Verlag GmbH & Co. KGaA, Weinheim [56].

Below LCST isolated particles showed a typical diameter of about 300 nm. Above LCST the microgels were found to be collapsed into a more compact appearance.

However, in both states a creased surface was observed.

In comparison, PNIPAAm microgels revealed a similar spherical shape, however, the outer diameter was found to be larger in case of the PVME microgels. The PNIPAAm particles tended to form aggregates in both the swollen and deswollen state (cf. Fig. 10) and revealed in the deswollen state a similar creased surface structure than PVME microgel particles.

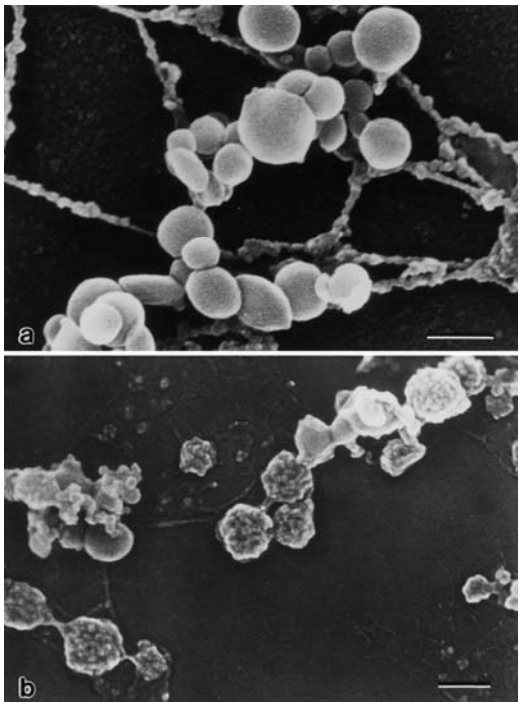

Fig. 10: PNIPAAm microgels synthesized by photo-crosslinking. The images show FESEM secondary electron micrographs below LCST at 25 °C (a) and above at 40 °C (b). The scale bars correspond to 100 nm. Reprinted with permission from Macromol Symp 210:501-511, R. Reichelt et al. Copyright (2004) Wiley-VCH Verlag GmbH & Co. KGaA, Weinheim [56].

In these presented studies, FESEM has proven to be a very suitable method for the structural characterization of PNIPAAm microgels. However, the determination of the particle size or the visualization of the particle distribution on a flat substrate can be studied also by SFM. For example, Sahiner at al. imaged cationic microgel particles attached to a flat mica surface by SFM operated in tapping mode [57]. Their sizes were measured to be in the range of 20 – 50 nm. Furthermore, light microscopy was used by the same group to image cationic microgels prepared with the fluorescein dye, thus showing that the oppositely charged microgel is strongly binding through electrostatic interactions.

Above mentioned examples demonstrate how different microscopy methods complementary contribute to the exploration of the swelling behaviour, the particle shape and the surface structure of microgels. Thus, profound insights gained by modern microscopies are followed by viable applications in many fields. In particular temperature-sensitive microgels based on PNIPAAm have tremendous importance in biotechnology. For example, PNIPAAm microgels may serve as a support substance for biological testing: In particular, oligodeoxiribonucleotides (ODN) may be attached to PNIPAAm microgels. The particles so-prepared were found to have an affinity for specific DNA due to their hydrophobic / hydrophilic property [58]. Another application used the very rapid swelling-shrinking-response of PNIPAAm microgels upon temperature change, thus allowing a drug to be temperature-controlled released. For example, fluorescein labelled dextran attached to PNIPAAm microgels is released when increasing the temperature above LCST [59]. Finally, Weissman et al. proposed an array of microgel particles to induce temperature-sensitive Bragg diffraction, finding applications in non-linear optics [60].

Filled Hydrogels

The swelling and deswelling of a temperature-sensitive hydrogel depends on a direct contact of the gel to a heat source or the heating and cooling of the surrounding liquid environment. Thus, the incapacity of changing the environmental temperature quickly hampers fast stimulation-reaction pathways. Some efforts are carried out to enhance the temperature setting in the very near of the polymer matrix. In particular, different hydrogels may be prepared in the presence of ferroelectric and ferromagnetic materials [61]. For example, barium

titanate (BaTiO3) and poly(vinylidene fluoride) (PVDF) as ferroelectric particles and Ni powder as ferromagnetic particles can be incorporated in the polymer matrix as "fillers". An alternating electric or magnetic field leads to a heating of the particles, thus influencing the swelling behaviour directly. Filling of hydrogels leads to materials with strongly modified characteristics [62,63,64]. In the above presented study, the fillers are incorporated in a PVME matrix and fixed either because of the size (the mesh size of the gel was observed to be smaller than the particles) or covalent bonding (in case of PVDF). FESEM proves also in this case to be perfectly suited to study the location of Ni, BaTiO3, and PVDF particles in the PVME hydrogels in the swollen and the deswollen state at high resolution (cf. Fig. 11).

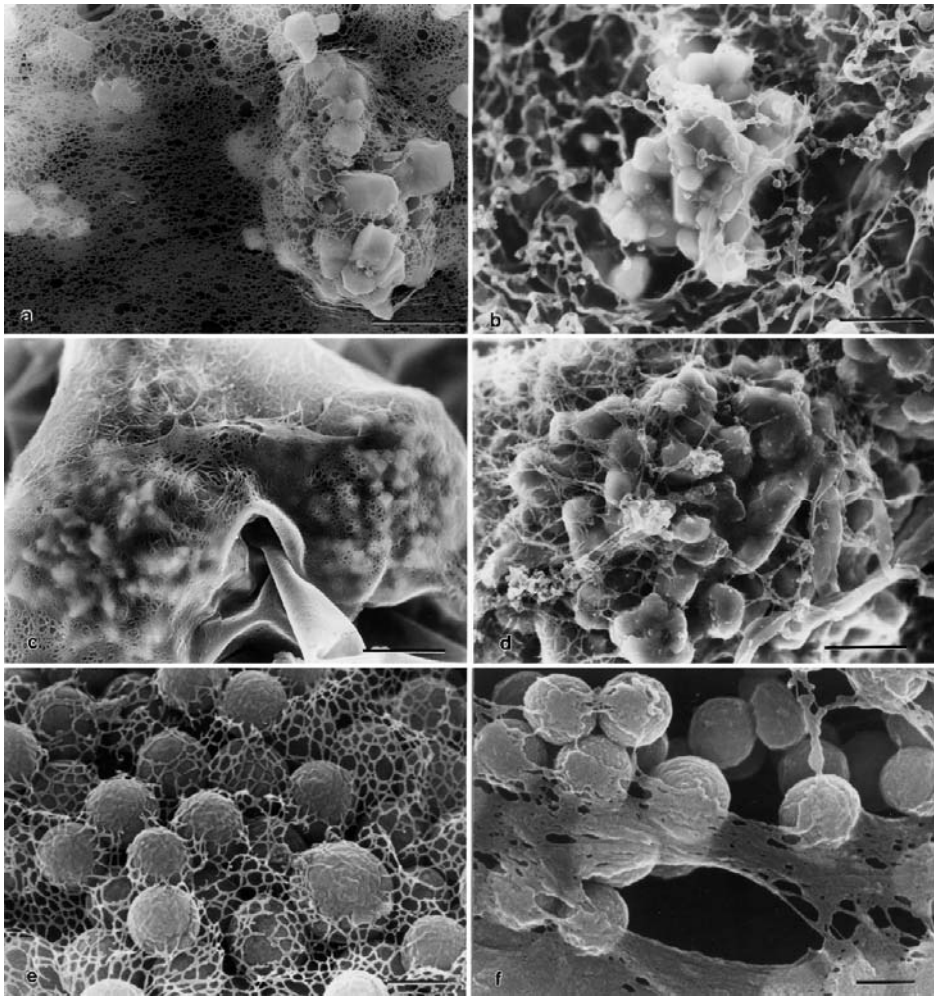

Fig. 11: PVME hydrogels filled with BaTiO3 (a, b), Ni (c, d), PVDF (e, f) in the swollen (left) and deswollen state (right). The images are FESEM secondary electron micrographs. The bars correspond to 1 µm (a-d) and 0.2 µm (e, f), respectively. The figure is a courtesy of D. Thesis et al. Reprinted with permission from J Appl Polym Sci 98:2253-2265, Copyright (2005) Wiley Periodicals, Inc. [61].

The uppermost PVDF spheres seem to be partially "coated" by a thin PVME layer. This appearance reminds of PNIPAAm coated spheres for drug release, reported by Ichikawa and Fukumori [65]. They created hydrogel particles that consist of a PNIPAAm shell surrounding a 100 µm drug release microcapsule. The shrinkage of the PNIPAAm shell most likely caused many voids in the coat and thereby imparted an enhanced water-

permeability. It was found that the hydrogel enables an "on-off" pulsatile release, which could alter the release in the order of a minute.

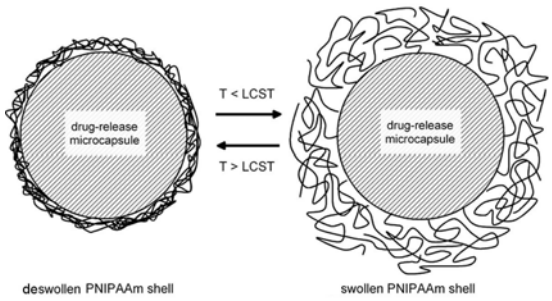

Fig. 12: Scheme of the PNIPAAm coated spheres below and above LCST.

DISCUSSION AND CONCLUSIONS

Scanning electron microscopy is widely used in the structural research of soft materials. Since about two decades, the so-called Environmental Scanning Electron Microscope (ESEM) allows wet matter to be studied at low vacuum (up to ~ 10 torr) of the operator's choice [66,67]. Common gaseous environment of wet specimens is water vapour, however, gasses like argon and nitrogen can also be used and may offer some advantages [68]. The ionization of the gas reduces the electric charge build-up that occurs on insulators being probed, thus, special sample preparation, especially conductive coating, is not needed. These findings might lead to the assumption that ESEM should be a suitable choice for studying the structure of water-swollen gels. Among a very few studies, e.g. Zhao et al. imaged the macroporous structure of PNIPAAm with an ESEM [40]. However, since wet hydrogels as well as microgels are mechanically sensitive structures, the polymer matrix can be deformed or may even collapse due to the effect of surface tension of water when decreasing the water level, thus hampering the observation of the real structure. To judge this surface tension induced effect of water during the process of air-drying, the forces should be estimated quantitatively [69]. Estimates of the forces are made in the following for a sphere and a thin beam (Fig. 13), which represent simple structures and fine structural elements of more complex structures, respectively.

The surface tension γ acts along the periphery of the structure. The length l of the periphery amounts for the sphere $l_{sp} = 2 \cdot \pi \cdot R$ and for the thin beam (Fig. b) $l_{beam} \approx 2 \cdot L$ (L >> thickness of the beam), respectively. Consequently, the force F pressing the structure towards the support amounts for the sphere $F_{sp} = l_{sh} \cdot \gamma \cdot \cos \vartheta$ and for the beam $F_{beam} = l_{beam} \cdot \gamma \cdot \cos \vartheta$, where ϑ denotes the contact angle of the water meniscus with the surface of the structure. The surface tension of water at 21 °C is $\gamma = 72.6 \frac{dyn}{cm}$ [70], (equal to 0.726 mN/cm).

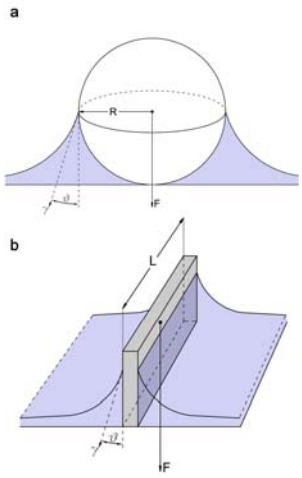

Fig. 13: Schemes of acting forces induced by the surface tension on the model structures sphere (a) and beam (b). Abbreviations: R – radius, γ – surface tension, F – force, ϑ - contact angle of the water meniscus, L – length of the beam, h – width of the beam, t – thickness of the beam, s – bending deflection.

The maximum induced force is applied if ϑ = 0 and amounts for a sphere with a diameter of 10 nm $F_{sh}^{\max} \approx 2.3\ nN$ and a corresponding pressure $p = \frac{F_{sp}^{\max}}{\pi R^2} \approx 300 \frac{kp}{cm^2}$ towards the support! The maximum induced force $F_{beam}^{\max}$ for a thin beam with a length of 100 nm amounts about 15 nN. It should be

mentioned that surface tension induced forces for other structures than sphere and beam with comparable size are in the same order of magnitude.

The deformation of a structure by forces depends on mechanical properties like the Young´s modulus E, its shape as well as the direction and the strength of the acting force. For a rough estimate of the deformation of individual structural features induced by surface tension we may consider two simple cases discussed in numerous textbooks of mechanics (e.g., Ashley [71]):

(i) The thin beam is fixed at one end and loaded with the force F at the other end (see Fig. 14). The bending deflection s at the end according to the textbooks is given as:

$$s = \frac{4F}{E} \cdot \frac{L^3}{th^3} \quad , \qquad (3)$$

where t is the thickness and h the width of the thin beam (F acts parallel to h; cf. Fig. 14). Considering the maximum force being generated by the surface tension acting along the full length L of the thin beam, we obtain for the bending deflection

$$s = \frac{6\gamma}{E} \cdot \frac{L^4}{th^3} \quad . \qquad (4)$$

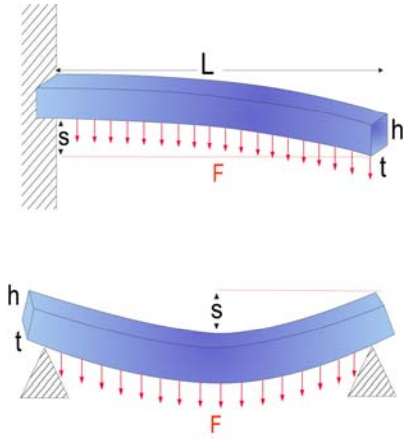

Fig. 14: Acting forces cause a one-sided jammed beam and a two-sided supported beam to bend by the bending deflection s. Abbreviations: see caption of Fig. 13.

(ii) The thin beam is fixed at both ends and loaded with the force F at the middle (see Fig. 14). The bending deflection s at the middle is given as

$$s = \frac{F}{4E} \cdot \frac{L^3}{th^3} \quad . \qquad (5)$$

The bending deflection induced by the surface tension, which acts along the full length of the thin beam is given for $\vartheta = 0$ by

$$s = \frac{3\gamma}{8E} \cdot \frac{L^4}{th^3} \quad , \qquad (6)$$

where F acts parallel to h as in case (i).

The equations (4) and (6) show that Young´s modulus is inversely proportional to the deformation and that the geometric parameters length and width effect very strongly the deformation because of their exponential contributions. The ratio of eq. (4) and (6) amounts 16, i.e., the bending is 16 times larger in case (i).

Table I gives a few numerical estimates. Experimental values used for calculation are based on data taken from FESEM micrographs (see Fig. 5) and from ESEM micrographs obtained by Zhao et al. [40]. To estimate the deformation of PNIPAAm beams, Young's modulus for the dry PNIPAAm gel is chosen (E = 791 kPa [41]), since the experimental data already include the effect of pores.

Table. I: Data used for calculation and estimated deformations for two simple cases, using equations (4) and (6). *A contact angle ϑ = 89.4° was used for the estimate.

	L	h	t	 bending deflection s [µm]	 bending deflection s [µm]
Microporous PNIPAAm (FESEM)	100 nm	100 nm	10 nm	$5.5 \cdot 10^{-2}$ *	$3 \cdot 10^{-3}$ *
Mesoporous PNIPAAm (ESEM)	50 µm	50 µm	2 µm	0.275	0.017

The above estimates prove ESEM being critical in case of hydrogel imaging in the water-swollen state, since features sticking out of the water can be artificially deformed. The deformation of the simple hydrogel structures reveals very high values for the deformation of thin PNIPAAm structures which may exeed the range of deformation where the elastic theory holds. However, the

estimates demonstrate that even forces below the maximum force ($0 < \vartheta < 90°$) are sufficient to induce significant structural deformations. In particular, submicrometer structures of soft matter are most sensitive to acting forces!

The surface tension does not induce hydrogel deformation if the hydrogel is completely embedded in water, i.e. no features are sticking out of the water. Imaging of the hydrogel in water with secondary electrons would not be sufficient since secondary electrons (SE) usually arise from a depth below approximately 10 nm, i.e. there is no access to information about the immersed hydrogel. In contrast to that, backscattered electrons (BSE) with an energy of 30 keV arise from a depth of a few micrometer in water [68], thus carrying information about structures some micrometers beneath the liquid surface. However, BSE imaging of very small hydrogel structures immersed in water seems impossible since the expected resolution is only about 100 nm or slightly better [72]. Moreover, the effective atomic number of water is according to Joy et al. [72] in the range of 3.1 - 4.4, which is very similar to the mean atomic number of PNIPAAm and other hydrogels too. Therefore, no significant atomic number contrast can be expected under these conditions.

In the quest for suitable methods in the micro-structural research of hydrogels, critical notes may also follow in case of SFM imaging. As yet there are no highly resolved topography images of hydrogel surfaces reported so far. About ten years ago Heuberger et al. [44] studied theoretically the resolution between Young's modulus and the obtainable resolution of SFM imaging. According to their results no high resolution imaging of soft matter can be obtained in contact mode due to a large contact area of the SFM tip. Therefore more gentle operation modes such as "dynamic scanning force mode (DSFM)", "tapping mode (TM)", "intermittend contact mode (IC-SFM)" or "jumping mode (JM)" were developed. These operating modes reduce the interaction time due to the short tip-sample contact. In spite of excellent results in studies of delicate samples like DNA molecules [73], a structural elucidation of the hydrogel surface remains hampered by a distinct surface corrugation. During scanning motion the cantilever tip may penetrate into pores and some more gel material gets in contact with the shaft of the tip.

In conclusion, information about the fine surface structures of wet hydrogels obtained by ESEM or SFM seems unreliable since the surface tension as well as imaging force may create artificially deformed structures. The HRSEM in combination with state-of-the-art cryo-preparation and thin conductive coating with an almost homogeneous Pt/C film are presently the only combination of techniques, which allow the structural characterization of hydrogels in different states down to a few nanometers.

The presented studies demonstrate some of the advantages and the strength of the complementary employment of FESEM and SFM in the characterization of soft materials: Highly resolved structural information by FESEM are complemented by SFM using micrometer-sized probing spheres for quantitative measurements of the local micromechanical properties of gels.

REFERENCES

[1] Wichter O., Lim D. (1960) "Hydrophilic Gels for Biological Use" *Nature* 185:117-118

[2] Okano T. (1998) *Biorelated Polymers and Gels. Controlled Release and Applications in Biomedical Engineering*, Boston, Academic Press

[3] Tanaka T. (1978) "Collapse of Gels and the Critical Endpoint" *Phys Rev Lett* 40:820-823

[4] Peppas N.A., Bures P., Leobandung W., Ichikawa H. (2000) "Hydrogels in pharmaceutical formulations" *Eur J Pharm Biopharm* 50:27-46

[5] Horare T.R., Kohane D.S. (2008) "Hydrogels in drug delivery: Progress and Challenges" *Polymer* 49:1993-2007

[6] Andrieux C.P, Audebert P, Bacchi P, Davisia-Blohorn B. (1995) "Kinetic behaviour of an amperometric biosensor made of an enzymatic carbon paste and a Nafion® gel investigated by rotating electrode studies" *J Electro Chem* 394:141-148

[7] Lin K., Bartlett S.P., Matsuo K., LiVolsi V.A, Parry C, Hass B, Whitaker, L.A. (1994) "Hyaluronic acid-filled mammary implants: an experimental study" *Plast Reconstr Surg* 94:306-315

[8] Osada Y, Kajiwara K. (2001) *Gels Handbook Vol. 3 Applications,* San Diego, Academic Press, pp. 4-19

[9] Verall M.S. (1996), *Processing of Natural Products*, Chichester, John Wiley & Sons, 159

[10] Ahn S.-K., Kasi R.M., Kim S.-C., Sharma N., Zhou Y. (2008) "Stimuli-responsive polymer gels" *Soft Matter*, DOI:10.1039/b714376a

[11] Tanaka T., Nishio I., Sun S.-T., Ueno-Nishio S. (1982) "Collapse of gels in an electric field" *Science* 218:467-469

[12] Kawasaki H., Sasaki S., Maeda H. (1997) "Effect of pH on the volume phase transition of copolymer gel of N-isopropylacrylamide and sodium acrylate" *J Phys Chem B* 101:5089-5093

[13] Esser-Kahn A.P., Francis M.B. (2008) "Protein-Cross-Linked Polymeric Materials through Site-Selective Bioconjugation" *Angewandte Chemie*, DOI: 10.1002/ange.200705564

[14] Cao Z., Du B., Chen T., Li H., Xu J., Fan Z. (2008) "Fabrication and Properties of Thermosensitive Organic/Inorganic Hybrid Hydrogel Thin Films" *Langmuir*, DOI:10.1021/la8000653

[15] Yoshida R., Uchida K., Kaneko Y., Sakai K., Kikushi A., Sakurai Y., Okano T. (1995) "Comb-type grafted hydrogels with rapid deswelling response to temperature changes" *Nature* 374:240-242

[16] Hirokawa Y., Tanaka T. (1984) "Volume phase transition in a nonionic gel" *J Chem Phys* 81:6379-6380

[17] Tanaka T., Fillmore D., Sun S.-T., Nishio I., Swislow G., Shah A. (1980) "Phase transitions in ionic gels" *Phys Rev Lett* 45:1636-1639

[18] Kiser P.F., Wilson G., Needham D. (1998) "A synthetic mimic of the secretory granule for drug delivery" *Nature* 394:459-462

[19] Yoshida R., Sakai K., Okano T., Sakurai Y. (1993) "Pulsatile drug delivery systems using hydrogels" *Adv Drug Deliv Rev* 11:85-108

[20] Park T.G., Hoffman A.S. (1993) "Thermal cycling effects on the bioreactor performances of immobilized β-galactosidase in temperature-sensitive hydrogel beads" *Enzyme Microb Technol* 15:476-482

[21] Holtz J.H., Asher S.A. (1997) "Polymerized colloidal crystal hydrogel films as intelligent chemical sensing materials" *Nature* 389:829-832

[22] Matsukata M., Takei Y., Aoki T., Sanui K., Ogata N., Sakurai Y., Okano T. (1994) "Temperature modulated solubility-activity alterations for poly(N-Isopropylacrylamide)-lipase conjugates" *J Biochem* 116:682-686

[23] Kanazawa H., Yamamoto K., Matsushima Y., Takai N., Kikuchi A., Sakurai Y., Okano T. (1996) "Temperature-responsive chromatography using poly(*N*-isopropylacrylamide)-modified silica" *Anal Chem* 68:100-105

[24] Osada Y., Okuzaki H., Hori H. (1992) "A polymer gel with electrically driven motility" *Nature* 355:242-244

[25] Kokufuta, E., and Aman, Y. (1997) "A biochemo-mechanical system consisting of polymer gels with immobilized glucose dehydrogenase" *Polym Gel Networks* 5, 439-454

[26] Peppas N.A., Zach Hilt J., Khademhosseini A., Langer R. (2006) "Hydrogels in biology and medicine: From molecular principles to bionanotechnology" *Adv Mater* 18:1345-1360

[27] Flory P.J. (1973) *Principles of Polymer Chemistry,*

Ithaca, New York, Cornell University Press

[28] Osada Y., Kajiwara K. (2001) *Gels Handbook Vol. 1: The Fundamentals,* San Diego, Academic Press, pp. 65-97

[29] Shibayama M., Shirotani Y., Hirose H., Nomura, S. (1997) "Simple Scaling Rules on Swollen and Shrunken Polymer Gels" *Macromolecules* 30:7307-7312

[30] Shirota H., Endo N., Horie K. (1998) "Volume phase transition of polymer gel in water and heavy water" *J Chem Phys* 238:487-494

[31] Takata S., Suzuki K., Norisuye T., Shibayama M. (2002) "Dependence of shrinking kinetics of poly(N-isopropylacrylamide) gels on preparation temperature." *Polymer* 43:3101-3107

[32] Suzuki A., Yamazaki M., Kobiki Y. (1996) "Direct observation of polymer gel surfaces by atomic force microscopy." *J Chem Phys* 104:1751-1757

[33] Matzelle T., Herkt-Buns Ch., Heinrich L.A., Kruse N. (2000) "Tribological properties of PNIPPAm" *Surf. Sci.* 454-456:1010-1015

[34] Wiedemair J., Serpe M.J., Kim J., Masson J.-F., Lyon L.A., Mizaikoff B., Kranz C. (2006) "In-situ AFM studies of the phase-transition behavior of single thermoresponsive hydrogel particles" *Langmuir* 23:130-137

[35] Li Y.Q., Tao N.J., Pan J., Garcia A.A., Lindsay S.M. (1993) "Direct measurement of interaction forces between colloidal particles using the scanning force microscope" *Langmuir* 9:637-641

[36] Ducker W.A., Senden T.J., Pashley R.M. (1992) "Measurement of forces in liquids using a force microscope" *Langmuir* 8:1831-1836

[37] Butt H.-J., Jaschke M., Ducker W. (1995) "Measuring surface forces in aqueous solution with the atomic force microscope" *Bioelectro* 38:191-201

[38] Hawkes P.W., Spence J.C.H. (2007) *The Science of Microscopy*, New York, Springer Science+Business Media, vol. 1, p. 235

[39] Kim S.H., Chu C.-C. (2000) "Pore Structure Analysis of Swollen Dextran-Methacrylate Hydrogels by SEM and Mercury Intrusion Porosimetry" *J Biomed Mater Res (Appl Biomater)* 53:258–266

[40] Zhao Q., Sun J., Zhou Q. (2007) "Synthesis of microporous poly(N-isopropylacrylamide) hydrogel with ultrarapid swelling-deswelling properties" *J Appl Polym Sci* 104:4080-4087

[41] Matzelle T.R., Ivanov D.A., Landwehr D., Heinrich L.A., Herkt-Bruns Ch., Reichelt R., Kruse N. (2002) "Micromechanical Properties of "Smart" Gels" *J Phys Chem B* 106:2861-2866

[42] Tao N.J., Lindsay N.M., Lees S. (1992) "Measuring the microelastic properties of biological material" *Biophys J* 63:1165-1169

[43] Weisenhorn A.L., Khorsandi M., Kasas S., Gotozos V., Celio M.R., Butt H.J. (1993) "Deformation and height anomaly of soft surfaces studied with an AFM" *Nanotech* 4:106-113

[44] Hoh J., Schoenenberger C.-A. (1994) "Surface morphology and mechanical properties of MDCK monolayers by atomic force microscopy" *J Cell Sci* 107:1105-1114

[45] Radmacher M., Fritz M., Hansma P.K. (1995) "Imaging soft samples with the atomic force microscope: gelatin in water and propanol" *Biophys J* 69:264-270

[46] Radmacher M., Fritz M., Kacher C.M., Cleveland J.P., Hansma P.K. (1996) "Measuring the viscoelastic properties of human platelets with the atomic force microscope" *Biophys J* 70:556-567

[47] Hertz H. (1882) "Über die Berührung fester elastischer Körper" *Journal für die reine und angewandte Mathematik* 9:156-171

[48] Heuberger M., Dietler G., Schlapbach L. (1996) "Elastic deformations of tip and sample during atomic force microscope measurements" *J Vac Sci Technol B* 14:1250-1254

[49] Munuera C., Matzelle T.R., Kruse N., López M.F., Gutiérrez A., Jiménez J.A., Ocal C. (2007) "Surface elastic properties of Ti alloys modified for medical implants: A force spectroscopy study" *Acta Biomat* 3:113-119

[50] Jacot J.G., Dianis S., Schnall J., Wong J.Y. (2006) "A simple microindentation technique for mapping the microscale compliance of soft hydrated materials and tissues" *J Biomed Mater Res A* 79:485-494

[51] Matzelle T.R., Geuskens G., Kruse N. (2003) "Elastic properties of poly-N-isopropylacrylamide and polyacrylamide hydrogels studied by Scanning Force Microscopy" *Macromolecules* 36:2926-2931

[52] Kuckling D., Harmon M.E., Frank C.W. (2002) "Photo-cross-linkable PNIPAAm copolymers. 1. Synthesis and characterization of constrained temperature-responsive hydrogel layers" *Macromolecules* 35:6377-6383

[53] Vo C.D., Kuckling D., Adler H.-J.P., Schönhoff M. (2001) "Preparation of thermosensitive nanogels by photo-cross-linking colloid" *Polym Sci* 280:400-409

[54] Pelton, R. (2000) "Temperature-sensitive aqueous microgels" *Adv Colloid Interface Sci* 85:1-33

[55] Arndt K.-F., Schmidt T., Reichelt R. (2001) "Thermo-sensitive poly(vinyl methyl ether) micro-gel formed by high energy irradiation" *Polymer* 42:6785-6791

[56] Reichelt R., Schmidt T., Kuckling D., Arndt K.-F. (2004) "Structural characterization of temperature-sensitive hydrogels by field emission scanning electron microscopy (FESEM)" *Macromol Symp* 210:501-511

[57] Sahiner N., Godbey W.T., McPherson G.L., John V.T. (2006) "Microgel, nanogel and hydrogel-hydrogel semi-IPN composites for biomedical applications: synthesis and characterization" *Colloid Polym Sci* 284:1121-1129

[58] Delair T., Meunier F., Elaissari A., Charles M.H., Pichot C. (1999) "Amino-containing cationic latex–oligodeoxyribonucleotide conjugates: application to diagnostic test sensitivity enhancement" *Colloids Surf A* 153:341-353

[59] Snowden M.J. (1992) "The use of poly(*N*-isopropylacrylamide) latices as novel release systems" *J Chem Soc Chem Comm* 803-804

[60] Weissman J.M., Sunkara H.B., Tse A.S., Asher S.A. (1996) "Thermally switchable periodicities and diffraction from mesoscopically ordered materials" *Science* 274:959-963

[61] Theiss D., Schmidt T., Dorschner H., Reichelt R., Arndt K.-F. (2005) „Filled temperature-sensitive poly(vinyl methyl ether) hydrogels" *J App Polym Sci* 98:2253-2265

[62] Gao L., Zhao X.J. (2004) "Electrorheological behaviors of barium titanate/gelatin composite hydrogel elastomers" *J Appl Polym Sci* 94:2517-2521

[63] Teixeira P., Azeredo J., Oliveira R., Chibowski E., Kato, N., Oishi, A., Takahashi, F. (1998) "Enzyme reaction controlled by magnetic heating due to the hysteresis loss of γ-Fe_2O_3 in thermosensitive polymer gels immobilized β-galactosidase" *Mater Sci Eng C* 6:291-296

[64] Kuckling D., Schmidt T., Filipscei G., Adler H.-J., Arndt K.-F. (2004) "Preparation of filled temperature-sensitive poly(*N*-isopropylacrylamide) gel beads" *Macromol Symp* 210:369-376

[65] Ichikawa H., Fukumori Y. (2000) "A novel positively thermosensitive controlled-release microcapsule with membrane of nano-sized poly(N-isopropylacrylamide) gel dispersed in ethylcellulose matrix" *J Control Rel* 63:107-119.

[66] Donald A.M. (1998) "Environmental scanning electron microscopy for the study of 'wet' systems." *Current Opinion in Colloid & Interface Science* 3:143-147

[67] Donald A.M. (2003) "The use of environmental scanning electron microscopy for imaging wet and insulating materials." *Nature Materials* 2:511-516

[68] Kadom A., Belkorissat R., Khelifa B. (2003) "Comparative study of electron beam-gas interaction in an SEM operating at pressures up to 300 Pa." *Vacuum* 69:537-543

[69] Anderson T.F. (1952) "Stereoscopic studies of cells and viruses in the electron microscope" *The Amer. Naturalist LXXXVI*, 91-100

[70] Lax E. (ed.) (1967) *Taschenbuch für Chemiker und Physiker*, Springer-Verlag, Berlin, 607

[71] Ashby M.F. (2005) *Materials selection in mechanical design.* 3rd ed., Elsevier, Amsterdam

[72] Joy D.C., Joy C.S. (2006) SEM imaging in liquids - Some data on electron interactions in water. *J Microsc* 221:84-88

[73] Schaper A., Pietrasanta L.I., Jovin T.M. (1993) **"**Scanning force microscopy of circular and linear plasmid DNA spread on mica with a quaternary ammonium salt" *Nucleic Acids Research* 25:6004-6009.